Poly(3,4-ethylenedioxythiophene) and Polyaniline Bilayer Nanostructures with High Conductivity and Electrocatalytic Activity

Lijuan Zhang,* Hui Peng, Paul A. Kilmartin, Christian Soeller, and Jadranka Travas-Sejdic*

Polymer Electronics Research Centre, Department of Chemistry, University of Auckland, Private Bag 92019, Auckland, New Zealand

Received June 11, 2008; Revised Manuscript Received August 14, 2008

ABSTRACT: Bilayer nanostructured poly(3,4-ethylenedioxythiophene) (PEDOT) and polyaniline (PANI) conducting polymer composites have been successfully prepared by oxidative polymerization of the parent monomers, aniline (An) and 3,4-ethylenedioxythiophene (EDOT), in aqueous solutions of *p*-toluenesulfonic acid (*p*-TSA). As the first step, PANI nanofibers were obtained in the *p*-TSA solution using ammonium persulfate (APS) as the oxidant. Subsequently, PEDOT was coated onto the PANI nanofibers by the oxidative polymerization of EDOT to form PEDOT/PANI bilayer nanofibers. The resulting nanostructured material was characterized by SEM and a range of spectroscopic methods, which confirmed that the surface layer of the synthesized materials had features typical of chemically synthesized PEDOT. The presence of the PEDOT layer increased the room temperature electrical conductivity of the PEDOT/PANI nanocomposites by 2 orders of magnitude in comparison with the parent PANI nanofibers. Moreover, PEDOT/PANI nanocomposites on a glassy carbon electrode showed stronger electrocatalytic activity for the oxidation of ascorbic acid than PANI nanofibers.

Introduction

Conducting polymers have offered a new generation of materials that exhibit electrical and optical properties of metals and semiconductors, while retaining the mechanical properties and processing advantages of organic polymers.[1] Polyaniline (PANI), polypyrrole and polythiophene, and their respective derivatives, exhibit high chemical stability and have been the most extensively studied conducting polymers to date, from both a scientific and from a practical commercial point of view.[2−5] Nanostructures of conducting polymers have attracted much attention due to the significant effect of the nanostructuring on the physical properties of the materials.[6−9] To date, various morphologies of conducting polymers, such as films with micropores,[10] hollow micro/nanospheres,[11] nanotubes,[12] and nanofibers[13] have been reported in the literature. More recently, it has been shown that PANI nanostructures doped with *p*-toluenesulfonic acid (*p*-TSA) can be obtained through a self-assembly process during oxidative polymerization.[14] However, the room conductivity of the PANI was relatively low in the range of 10^{-2} S cm^{-1}. The electronic and optical properties of PANI can be improved by molecular engineering or by mixing with other materials (organic or inorganic compounds) in order to obtain composites.[15−18] Novel properties of composites can be derived from the successful combination of the characteristics of the parent constituents.[16,19] Poly(3,4-ethylenedioxythiophene) (PEDOT) is a particularly promising organic electrode material, which exhibits a number of desirable properties in the oxidized state, including high conductivity and excellent environmental stability.[20−22] The electrocatalytic oxidation of ascorbic acid has been demonstrated at PEDOT electropolymerised on glassy carbon[23,24] or platinum[25] electrodes. However, nanosize materials of PEDOT, such as nanowires and nanorods, of regular size and shape, are difficult to prepare without the use of external templates, in contrast to PANI.[22]

In this work, we demonstrate the preparation of bilayer nanostructured composites consisting of PEDOT and PANI by means of oxidative polymerization in aqueous solutions of *p*-TSA. This was achieved by first synthesizing PANI nanofibers and subsequent polymerization of EDOT onto the PANI nanofibers. The composites were characterized by SEM, TEM and a range of spectroscopic methods which revealed that the surface layer of the synthesized materials has features matching those of chemically synthesized PEDOT. The morphology, conductivity and electrocatalytic activity toward ascorbic acid (AA) oxidation of the PEDOT/PANI nanocomposites are evaluated.

Experimental Section

Materials. 3,4-Ethylenedioxythiophene (EDOT), Aniline (An), *p*-toluenesulfonic acid (*p*-TSA) and ammonium persulfate ($(NH_4)_2S_2O_8$, APS), and ascorbic acid (AA) were obtained from Aldrich Chem. Co. EDOT and aniline were distilled under reduced pressure and stored in the dark under nitrogen. The citrate/phosphate aqueous buffer at pH 3.0 was prepared by mixing 79.45 mL of 0.1 M citric acid and 20.55 mL of 0.2 M dibasic sodium phosphate (Na_2HPO4). The citrate/phosphate aqueous buffer at pH 6.0 was prepared by mixing 36.85 mL of 0.1 M citric acid and 63.15 mL of 0.2 M Na_2HPO4.

Synthesis of PANI Nanofibers. PANI nanofibers were synthesized by dissolving 0.2 M aniline and 0.1 M *p*-TSA in 10 mL of Milli-Q water at room temperature. The solution was cooled in a refrigerator at 5 °C for 30 min, after which 5 mL of a precooled aqueous solution of 0.4 M APS was added, to give an initial concentration of aniline and APS both = 0.133 M, and *p*-TSA = 0.067 M. The reaction was continued for a total of 16 h by which time a black-green precipitate of PANI had formed. The obtained PANI was filtered and the precipitate was washed with water, methanol and acetone several times. Finally, the product was dried in vacuum at room temperature for 24 h.

Synthesis of PEDOT/PANI Bilayer Nanofibers. PEDOT/PANI bilayer nanofibers were synthesized by using APS oxidant from the solution of 0.04−0.1 M EDOT and 0.5 M of *p*-TSA in the presence of PANI nanorods at room temperature. First, the 0.120 g of PANI nanorodes were dispersed in 40 mL 0.5 M *p*-TSA solution with stirring, then, 0.16 mL of the EDOT solution was dispersed in as well. The solution was kept stirring for an hour to disperse the EDOT very well. Finally, 0.3408 g APS in 20 mL of 0.5 M *p*-TSA solution was added. Stirring was maintained for 24 h

* Corresponding authors. Telephone: +64 9 373 7599ext. 88272. Fax: +64 9 3737422. E-mail: (L.Z.) lijuan.zhang@auckland.ac.nz; (J.T.-S.) j.travas-sejdic@auckland.ac.nz.

10.1021/ma8013228 CCC: $40.75
Published on Web 09/24/2008

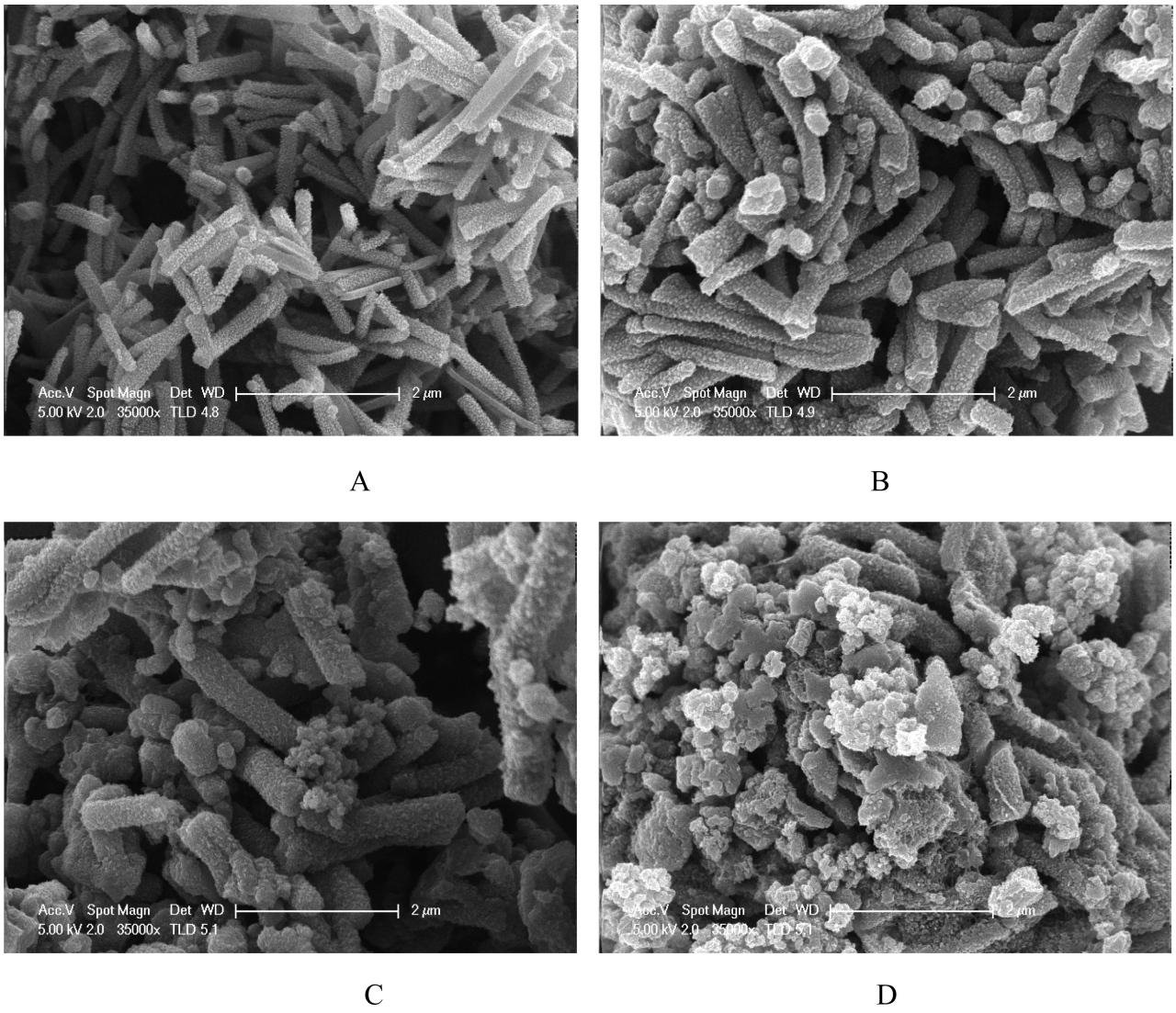

Figure 1. SEM images of PANI (A) and PEDOT/PANI obtained using different concentrations of EDOT: (B) 0.04 M, (C) 0.1 M and (D) 0.18 M.

throughout the experiment. The obtained product powder was filtered and washed with distilled water and acetronitrile several times, then dried in vacuum at room temperature for 24 h. In all of the experiments, the molar ratio of EDOT to APS was 1:1.[26,27] Different concentrations of *p*-TSA were used to investigate the influence of *p*-TSA concentration on the conductivity of the bilayer nanostructures.

SEM and TEM Characterization. The morphologies of the products were investigated using a Philips XL30S field emission scanning electron microscope (SEM) and a Philips CM12 transmission electron microscopy (TEM). The samples for SEM were mounted on aluminum studs using adhesive graphite tape and sputter-coated with platinum before analysis. For TEM measurements the samples were dispersed on microgrids copper coated with a carbon support film.

Spectroscopy. Various spectra were obtained for the PANI and PEDOT/PANI nanorods. The UV−visible absorption spectra of the products dissolved in DMSO were recorded from 250 to 1100 nm using a Shimadzu UV1700 UV−visible spectrophotometer. Infrared spectra in the range 400−4000 cm^{-1} were measured on pellets made with KBr by means of a Perkin-Elmer 1600 FTIR spectrophotometer, taking 10 scans at a resolution of 4 cm^{-1}. Raman spectra in the range 200−2000 cm^{-1} were collected for powder samples using a Renishaw microscope (RM-1000) and a 785 nm laser excitation wavelength. The X-ray scatting experiments were carried out on an X-ray diffraction instrument (Micscience M18XHF with a Cu Kα radiation). XPS measurements on the sample powders were made using a Kratos Axis Ultra spectrometer with an Al Kα source (1486.7 eV). The X-ray source was run at a reduced power of 150 W. The samples were mounted on standard VG sample studs by means of an indium wafer.

Conductivity. The room temperature conductivity of compressed pellets was measured by a standard four-probe method using a Jandel Model RM2 instrument. The samples were pelletized to a diameter of 1.5 cm and a thickness of 0.6 mm using a vacuum press at 8 MPa for 5 min.

Cyclic Voltammetry. The electrochemical response of the material was determined using a CHI440 (CH Instruments) electrochemical workstation. Each sample was first dispersed in ethanol and the dispersion was dropped onto a (BioAnalytical Systems) 3 mm diameter glassy carbon electrode to form a film which was allowed to dry at room temperature. Hydrochloric acid solution (0.5 M) and two different citrate/phosphate buffers (pH 3 and pH 6) were employed for the electrochemical investigation. Ascorbic acid additions to the buffer solutions were made immediately prior to use. All of the electrochemical experiments were made at room temperature. The solutions were purged with N_2 for approximately 10 min. Following this, N_2 was allowed to flow over the solution to prevent O_2 from re-entering the cell for the remainder of the experiment. Cyclic voltammograms were recorded at a scan rate of 50 mV s^{-1}, using an Ag/AgCl (+207 mV vs SHE) reference electrode and a Pt wire counter electrode.

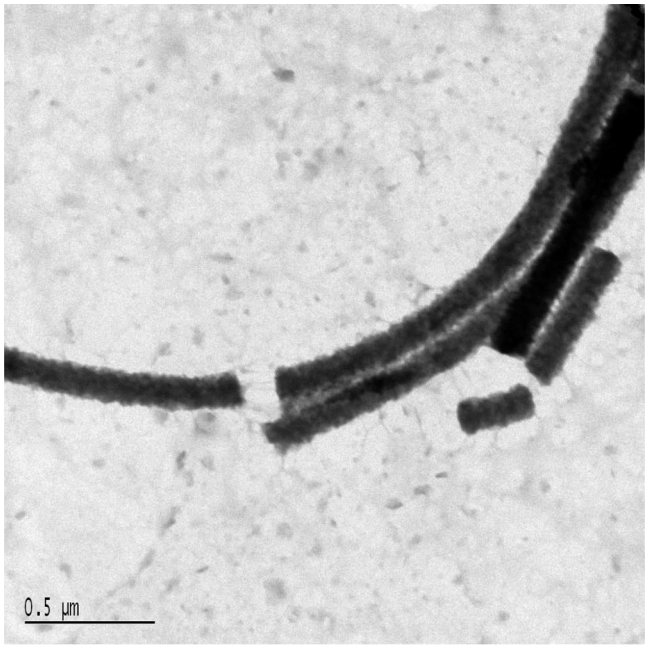

A

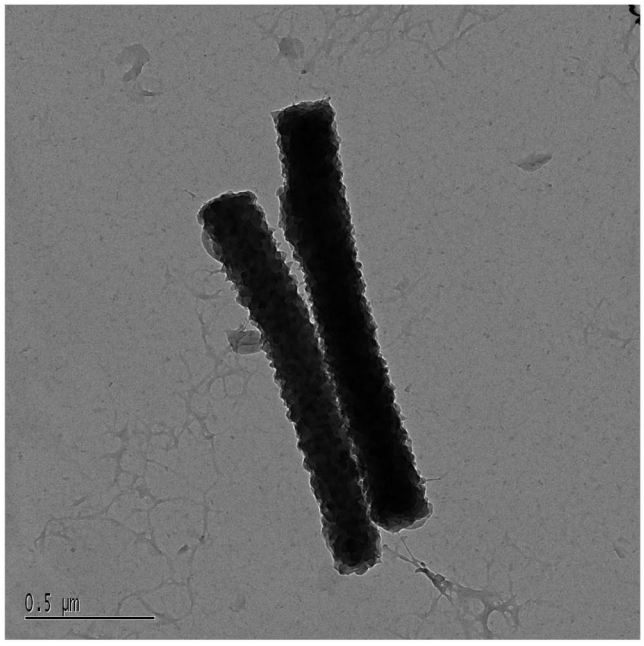

B

Figure 2. TEM images of PANI (A) and PEDOT/PANI (B) obtained using a 0.04 M EDOT concentration.

Results and Discussion

1. PEDOT/PANI Formation. On the basis of previous work, PANI nanofibers were prepared by oxidative polymerization of aniline from a solution containing *p*-TSA and APS whereby a nanofibrilar structure was developed through a self-assembly process.[14] Figure 1A presents a SEM image of the PANI nanofibers which had an average diameter of 170 ± 20 nm. Figure 1B−D shows SEM images of PEDOT/PANI nanofibers obtained after further polymerization of EDOT onto the PANI nanofibers from solutions of different concentrations of EDOT. It can be seen that the diameter of the PEDOT/PANI nanofibers increased as the concentration of EDOT moved from 0.04 M (Figure 1B), with 280 ± 30 nm fibers, to 0.1 M (Figure 1C), with 440 ± 40 nm fibers. The diameter of the PEDOT/PANI nanofibers obtained with the lowest investigated EDOT concentration was about 65% larger than the diameter of parent PANI nanofibers. However, when the concentration of EDOT was much higher (0.18 M, Figure 1D) a significant portion of free granular PEDOT was observed which was much less evident at the lower EDOT concentrations. Parts A and B of Figure 2 present TEM images of the PANI and PEDOT/PANI nanofibers, using a 0.4 M EDOT concentration. From these images, it can be clearly seen that the inner cores of the PANI and PEDOT/PANI nanofibers are indeed solid and that the diameter of PEDOT/PANI nanorods is larger than that of the PANI nanorods. The interface of the two polymer layers could not be seen due to the similar polymer properties of PANI and PEDOT.

On the basis of the above results, we propose the following scheme (Figure 3) for the PEDOT/PANI nanorod formation: for appropriately low concentrations of EDOT monomer the PEDOT preferentially polymerizes on the PANI nanorod templates. Prior to addition of the oxidant, the solution contains PANI nanorods, EDOT monomers, and *p*-TSA molecules. Most likely both EDOT monomer and *p*-TSA molecules adsorb on the surface of PANI nanofibers via hydrophilic, H-bonding and electrostatic interactions, facilitated by the high surface area of the PANI nanorods and low solubility of EDOT monomer in water. Upon addition of the APS oxidant, polymerization takes place on the surface of the PANI nanorods, increasing the diameter of the parent PANI nanorods; some EDOT oligomers formed in the solution could also adsorb onto the PANI nanorods. The diameter increase is proportional to the increase in EDOT concentration in the solution until a concentration of EDOT is reached such that the PANI nanorods cannot absorb all of the EDOT, and consequently granular PEDOT forms independently of the PANI nanorod templates.

2. Structural Characterization. The UV−vis absorption spectra of the PEDOT/PANI and PANI nanorods dissolved in dimethyl sulfoxide (DMSO) are shown in Figure 4. The absorption at 330 nm is assigned to a π-π^* excitation of the para-substituted benzene segment in PANI (−B−NH−B−NH−B−; B, benzenoid), which appeared in both of the PANI (Figure 4A) and PEDOT/PANI (Figure 4B) spectra[28] and became broader in the spectrum of PEDOT/PANI. The absorption at 630 nm is commonly attributed to the excitation of the quinone diimine structure (−*N*═Q═N−; Q, quinoid) in PANI,[29] which appeared as a peak in the spectrum of the PANI nanorods (Figure 4A) but was less apparent in the spectrum of PEDOT/PANI nanorods due to new PEDOT absorption bands (Figure 4B). A new broad shoulder absorption peak centered at 450 nm corresponding to the π-π^* transition of PEDOT and a broad absorption feature in the 700 to 900 nm range related to the charge-carrier band of PEDOT appeared in the spectrum of PEDOT/PANI[30,31] which therefore confirms the presence of PEDOT. It needs to be noted that the absorption peaks in the spectrum of PEDOT/PANI have some shift compared with the absorption peaks in the spectrum of pure PEDOT (Figure 4C), which may be caused by the morphology difference and the interaction of PANI with PEDOT.

The FTIR spectra of PEDOT/PANI and PANI nanorods are shown in Figure 5. Various bands typical of PANI were obtained as shown in Figure 5A. The characteristic PANI peaks at 1568 and 1488 cm^{-1} are attributed to the C═C stretching of quinoid and benzenoid rings, respectively.[32] The bands at 1298 and 1243 cm^{-1} are related to the C−N and C−$N^{+\bullet}$ stretching modes, the band at 1136 cm^{-1} is due to C−H in-plane bending, and the band at 802 cm^{-1} corresponds to the out-of-plane bending of C−H, which all appeared in the spectrum of the PANI nanorods.[32−36] The bands at 1043 and 508 cm^{-1} are assigned

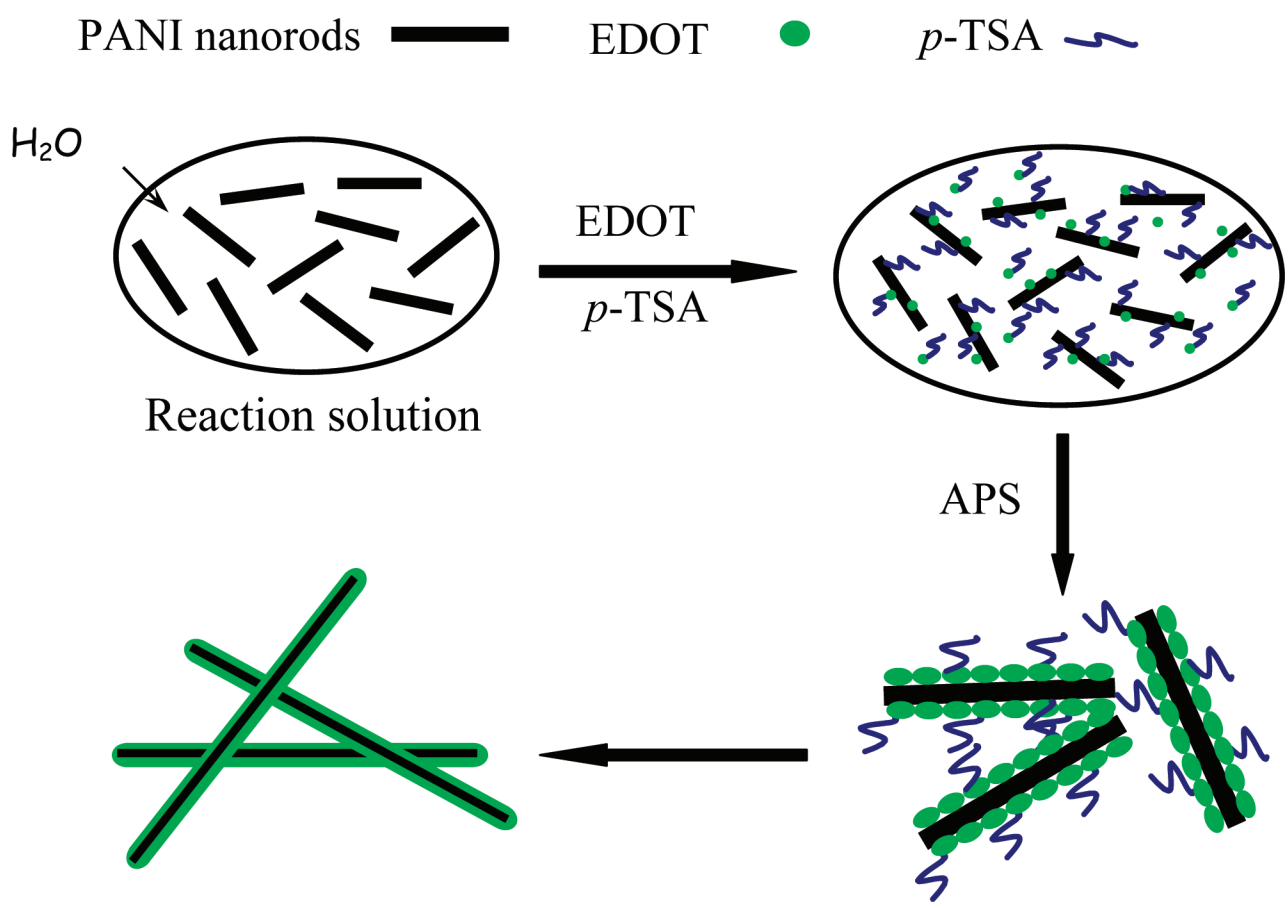

Figure 3. Proposed formation mechanism for the bilayer nanostructures of the PEDOT/PANI composites.

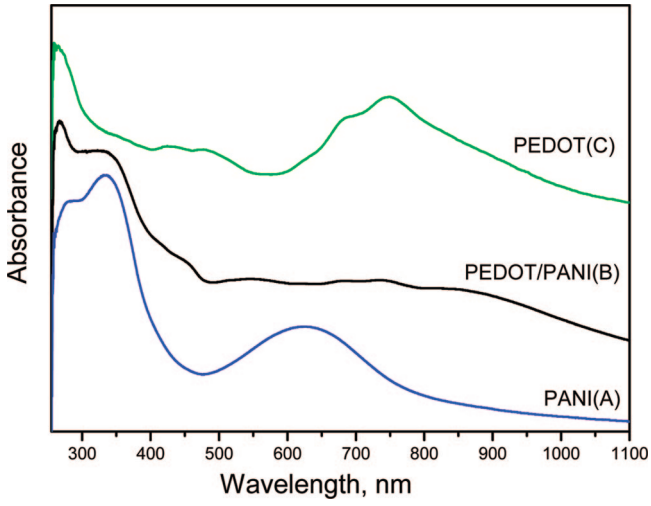

Figure 4. UV spectra of PANI (A) and PEDOT/PANI (B) nanorod samples and (C) a PEDOT sample in DMSO solution.

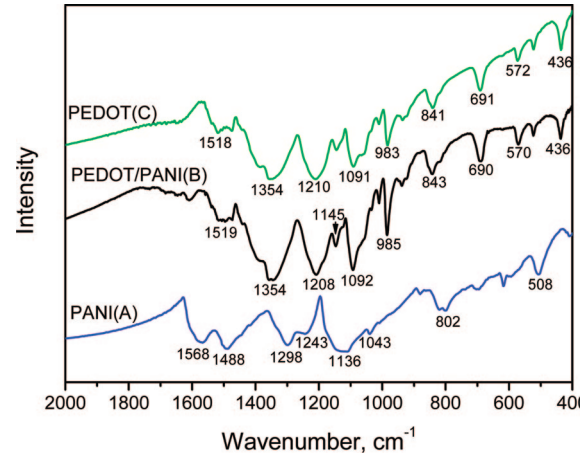

Figure 5. FTIR spectra of PANI (A) and PEDOT/PANI (B) nanorod samples and (C) a PEDOT sample.

to the vibrations of the $-SO_3H$ group, which confirms that the PANI nanorods are doped with *p*-TSA.[37] The FTIR features of PEDOT/PANI nanorods (Figure 5B) are consistent with the spectrum of PEDOT (Figure 5C). The vibrations at 1354 and 1519 cm^{-1} are due to C−C and C═C stretching of the quinoidal structure of the thiophene ring.[20] The vibrations at 1208, 1145 and 1092 cm^{-1} originate from C−O−C bond stretching in the ethylene dioxy (alkylenedioxy) group.[38] The C−S bond stretching in the thiophene ring is also seen at 985, 843, and 690 cm^{-1}.[39] The weak peak at 1043 cm^{-1} is attributed to the $-SO_3H$ group which suggests that the resulting PEDOT is in a doped state.[37] The FTIR spectra therefore confirm that the surface of the resultant nanorods is covered by a PEDOT layer.

Raman spectra of PEDOT/PANI and PANI nanorods, and a standard PEDOT powder sample, are shown in Figure 6. Typical characteristic bands of PANI chains were observed for the PANI nanorods (Figure 6B). The bands at 1599 and 1373 cm^{-1} are assigned to the C−C stretching vibration of the benzenoid and quinoid rings.[40,41] The bands at 1507, 1335, and 1172 cm^{-1} correspond to the N−H stretching mode, the C−N stretching of the cation radical and the C−H bending vibration, respectively.[41−43] The bands at 805 and 413 cm^{-1} relate to the C−H deformation, the band at 575 cm^{-1} is attributed to the amine deformation, and the band at 519 cm^{-1} is ascribed to the C−N−C torsion.[40,41] These bands imply that the polymer chains

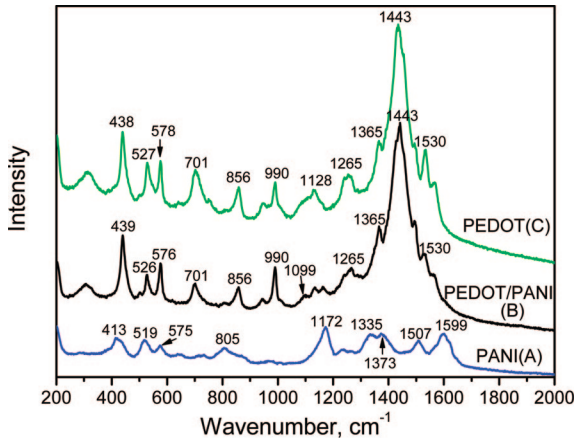

Figure 6. Raman spectra of PEDOT/PANI (A) and PANI (B) nanorod samples and (C) a PEDOT sample.

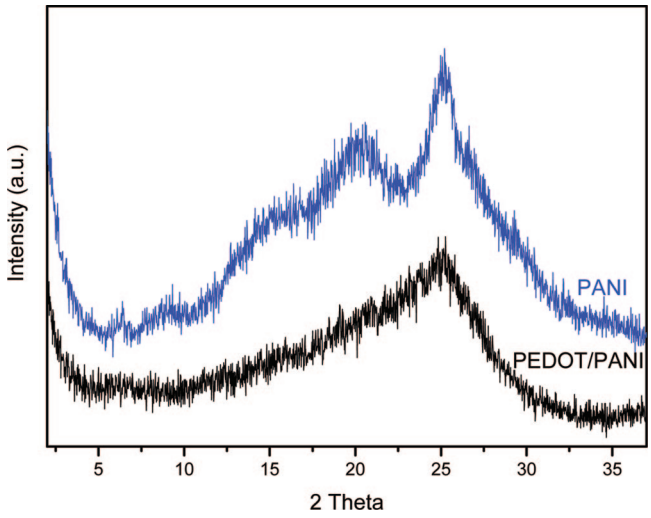

Figure 7. XRD curves of PEDOT/PANI (A) and PANI (B) nanorod samples.

of the PANI nanorods are conventional PANI. The Raman spectrum of the PEDOT/PANI nanorods (Figure 6A) is similar to PEDOT (Figure 6C) synthesized using conventional methods.[44−47] The shoulder band at 1530 cm^{-1} is associated with the $C_\alpha{=}C_\beta$ antisymmetric stretching vibration,[46,48] whereas the most intense band at 1443 cm^{-1} is assigned to the symmetric stretching mode of the aromatic $C_\alpha{=}C_\beta$ bond.[44] The 1365 and 1265 cm^{-1} bands are attributed to the stretching modes of single $C_\alpha{-}C_{\alpha'}$ bonds and the $C_\alpha{-}C_{\alpha'}$ inter-ring bonds, respectively.[49] The bands at 990 and 576 cm^{-1} are attributed to the oxyethylene ring deformation, while the band at 701 cm^{-1} is related to the symmetric C−S−C deformation.[46] It needs to be noted that the band at 526 cm^{-1}, which is usually associated with defects in the polymer chains, becomes weaker in the Raman spectrum of PEDOT/PANI compared with the spectrum of pure PEDOT, suggesting that the PEDOT chains are highly regular and possess a more highly conjugated structure due to the nanostructuring of the PEDOT/PANI composite.[44] This is additionally confirmed by the presence of a weak band at 1099 cm^{-1} related to the distorted C−C inter-ring bonds of the polymer chains.[44] The Raman spectra therefore also confirm that the surface of PEDOT/PANI nanorods was fully covered by a PEDOT layer.

Figure 7 shows the X-ray diffraction patterns of PANI and PEDOT/PANI nanorods respectively. Four peaks centered at $2\theta = 6.48°$, 9.16°, 20.1°, and 25.1° were observed for the PANI nanorods. In general, the first peak at 2θ6.48° is assigned to the periodicity distance between the dopant and N atom on

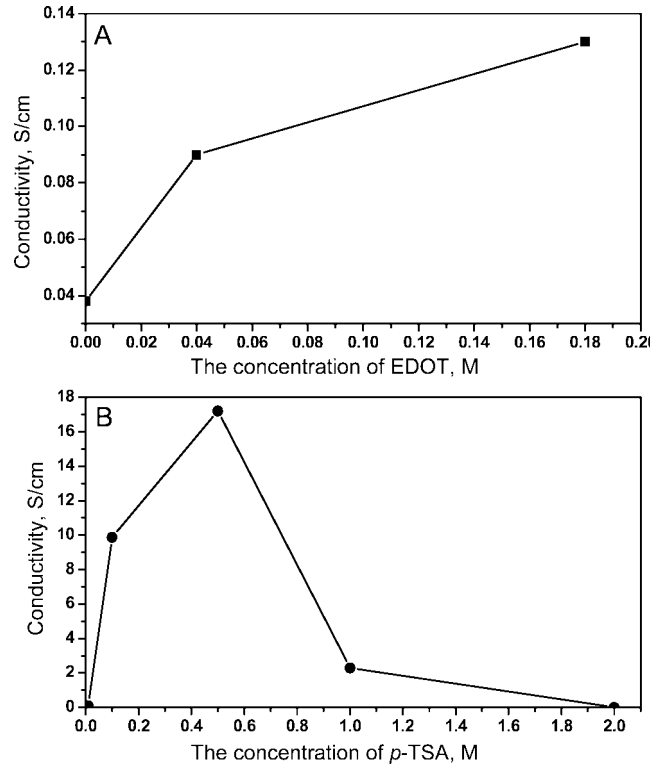

Figure 8. (A) Impact of EDOT concentration on the room-temperature conductivity of PEDOT/PANI nanorods at a *p*-TSA concentration of 0.01 M; and (B) impact of *p*-TSA concentration on the room-temperature conductivity of PEDOT/PANI nanorods at an EDOT concentration of 0.04 M.

adjacent main chains.[50] The second peak at 2θ9.16° is assigned to the repeat unit of the polymer chains, while the later two bands are ascribed to the periodic parallel and perpendicular features of the polymer chains of PANI.[51,52] After coating of the PANI nanorods with PEDOT, only one broad peak centered at 25°was observed, which most likely corresponds to the thiophene rings perpendicular to the layer due to amorphous structures of the PEDOT layer[53] based on the absence of the peaks at 2θ6.48°, 9.16°, and 20.1° that originated from PANI. Therefore, the result of XRD patterns indicates that the surface of the PEDOT/PANI nanorods is largely covered by a PEDOT layer.

We have also tested the PANI and PEDOT/PANI materials using XPS, and the N 1s peak due to PANI completely disappeared in the XPS spectrum of PEDOT/PANI materials, again confirming the full coverage of the PANI nanorods with a PEDOT layer.

3. Electrical Properties and Electrocatalytic Activities. The room temperature conductivity of the samples was measured using a standard four-probe method. The measured conductivity of a pellet of PANI nanorods was 3.8×10^{-2} S cm^{-1}, while the conductivity of PEDOT/PANI nanorods increased from 9.0×10^{-2} S cm^{-1} to 1.3×10^{-1} S cm^{-1} with an increase of EDOT concentration from 0.04 to 0.18 M, at a *p*-TSA concentration of 0.01 M (Figure 8A). The reason maybe the contribution of the thicker outer PEDOT layer with an increase of EDOT concentration. As shown in Figure 8B, the conductivity also increased from 9.0×10^{-2} S cm^{-1} to 17.2 S cm^{-1} when the concentration of *p*-TSA was increased from 0.01 to 0.5 M at an EDOT concentration of 0.04 M. However, the conductivity of the composite nanostructures decreased from 2.3 S cm^{-1} to 7.5×10^{-3} S cm^{-1} when the concentration of *p*-TSA was increased from 1 to 2 M. The conductivity decrease with increasing *p*-TSA concentration was most likely resulted from

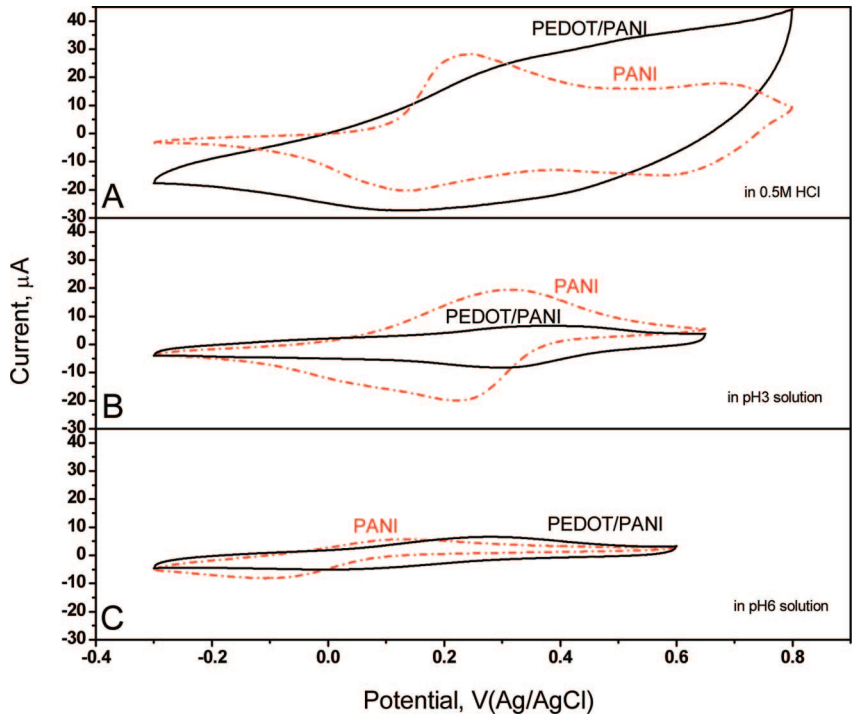

Figure 9. Cyclic voltammograms of PEDOT/PANI and PANI nanostructures cast on a glassy carbon electrode in the different solutions: (A) 0.5 M HCl and (B) pH 3 and (C) pH 6 citrate/phosphate buffer solutions, at a scan rate of 50 mV s^{-1}.

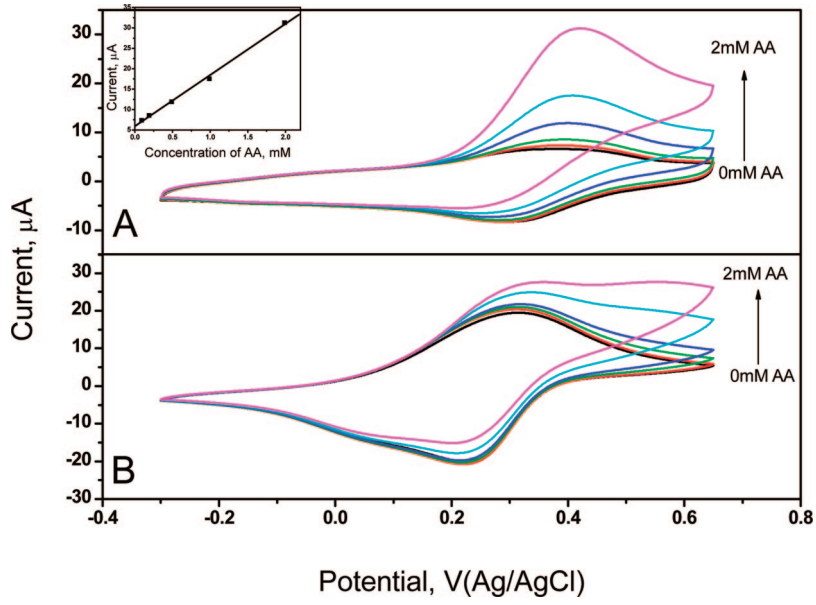

Figure 10. Cyclic voltammograms of PEDOT/PANI (A) and PANI (B) nanostructures cast on a glassy carbon electrode in the presence of ascorbic acid at concentrations 0, 0.1, 0.2, 0.5, 1 and 2 M, in a pH 3 citrate/phosphate buffer solution at a scan rate of 50 mV s^{-1}. Inset in part A: Plot of anodic current versus ascorbic acid concentration at 0.42 V for the PEDOT/PANI system.

excess *p*-TSA that EDOT polymerization kinetics slows down at pH lower than 2.7 and there is a higher probability of degradative reaction taking place.[26]

The electrochemical characteristics of the PEDOT/PANI and PANI nanorods were investigated by cyclic voltammetry. Samples of both PANI nanorods and the highly conductive PEDOT/PANI obtained from the reaction solution using 0.04 M of EDOT and 0.5 M of *p*-TSA was dispersed in ethanol and drop-cast onto a glassy carbon electrode. Figure 9 shows the cyclic voltammograms (CVs) of PEDOT/PANI and PANI nanorod films as the electrode was cycled in different pH solutions at a scan rate of 50 mV s^{-1}. As shown in Figure 9A when the PANI nanorod film was cycled in 0.5 M HCl (pH = 1) there were two sets of redox peaks in agreement with the expected electrochemical behavior of PANI.[47,48] The oxidation process with a peak at approximately +240 mV is due to the oxidation of the leucoemeraldine to the emeraldine form of PANI, and the peak at approximately +680 mV is due to oxidation from the emeraldine to the pernigraniline form.[54,55] After coating with PEDOT, the two peaks characteristic to PANI could not be distinguished from the broad oxidation and reduction curves which likely included the redox response of PEDOT in addition to PANI. In a pH 3 buffer solution, the two sets of PANI peaks overlapped into a single set of redox peaks and a lower overall current response, with an oxidation peak seen at +310 mV for the oxidation of the leucoemeraldine

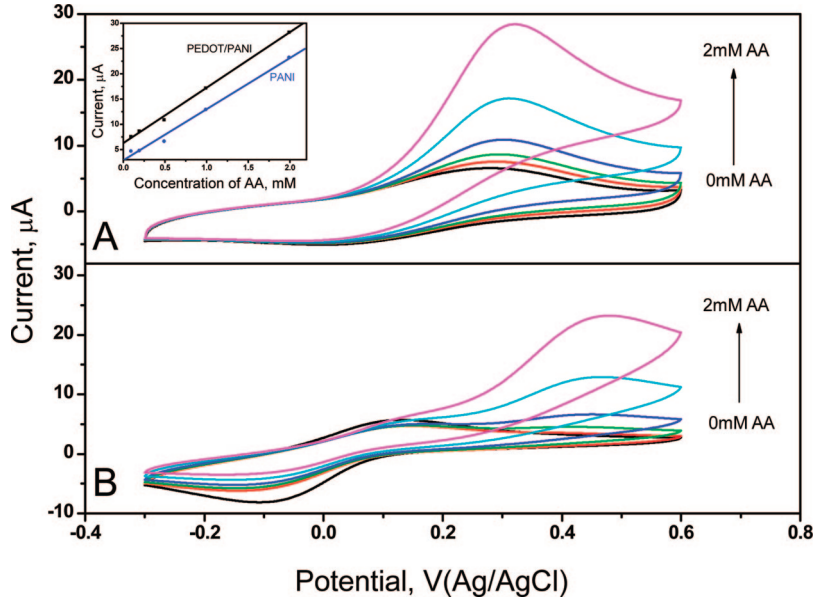

Figure 11. Cyclic voltammograms of PEDOT/PANI (A) and PANI (B) nanostructures cast on a glassy carbon in the presence of ascorbic acid at concentrations 0 0.1, 0.2, 0.5, 1m and 2 M, in a pH 6 citrate/phosphate buffer solution at a scan rate of 50 mV s^{-1}. Inset in part A: Plot of anodic current versus ascorbic acid concentration at 0.32 V for PEDOT/PANI and at 0.48 V for the PANI system.

through to the pernigraniline form (Figure 9B).[56] The dependence of PANI electrochemistry upon solution pH is well-known.[57,58] A redox wave with an oxidation peak at +380 mV in the CV of PEDOT/PANI nanorods at pH 3 is again expected to represent the combined electrochemical contributions of PEDOT and PANI. When a pH 6 buffer solution was used for electrochemical cycling, the currents became even smaller (Figure 9C). A redox wave with an oxidation peak at +280 mV that belongs to PEDOT appeared in the voltammogram of PEDOT/PANI, a positive shift from the position of the redox wave for PANI with an oxidation peak at +130 mV.

Parts A and B of Figure 10 show the CVs of PEDOT/PANI and PANI nanorods in the presence of different concentrations of ascorbic acid (AA) at pH 3 (citrate/phosphate buffer aqueous solution). As shown in Figure 10B, additional current at potentials greater than 0.2 V pointed to the ability of ascorbic acid to reduce the partially oxidized PANI nanorod film, which could then be oxidized again at the glassy carbon electrode - an electrocatalytic effect.[59] In the absence of a conducting polymer film, ascorbic acid is only oxidized at more positive potentials. On the return voltammogram with the PANI nanorods, a significant polymer reduction peak could still be seen, showing that the ascorbic acid, even at a concentration of 2 mM was only reducing a small fraction of the PANI nanorods in contact with the glassy carbon electrode in the time frame of the experiment. By contrast, a larger catalytic current was generated with the PEDOT/PANI film (Figure 10A) with a definite peak observed at about +420 mV, showing the stronger electrocatalytic activity to AA of the PEDOT/PANI film. The oxidant peak current increased at higher AA concentrations in a linear fashion (inset in Figure 10A) in the AA concentration range of 0.1−2 mM, with a correlation coefficient of 0.9988. This rapid and complete reduction of PEDOT/PANI by AA was also seen in the very small cathodic current obtained on the reverse sweep in the voltammograms (Figure 10A), particularly with the higher strength (2 mM) AA solution.

Further investigation was carried out at the scan rate of 50 mV s^{-1} in a pH 6 citrate/phosphate buffer aqueous solution for different concentrations of AA. At pH 6 PANI is expected to be less electroactive than at pH 3, while ascorbic acid is more easily oxidized.[59] Parts A and B of Figure 11 give the CVs of PEDOT/PANI and PANI for different concentrations of AA in the pH 6 citrate/phosphate buffer aqueous solution. Both the PANI and PEDOT/PANI nanostructures showed an oxidantion peak which increased linearly with AA concentration in the range of 0.1−2 mM; the correlation coefficients were 0.9987 and 0.9954 respectively for PEDOT/PANI and PANI cast film electrodes. In this case the onset of ascorbic acid oxidation occurred at a lower electrode potential for PEDOT/PANI compared to PANI alone, indicating that the addition of PEDOT had lowered the overpotential for the AA oxidation process. The AA oxidation peak potential also shifted negatively from +480 mV to +320 mV and the peak current increased from 23 to 28 μA for the PEDOT/PANI cast film electrode compared to the PANI film for 2 mM AA. This further confirms that the PEDOT/PANI cast film electrode showed a more effective electrocatalytic activity for AA oxidation.

Conclusions

PANI nanorods were used as templates for the synthesis of PEDOT nanorods, illustrating a synthetic method for obtaining conducting polymer nanostructures which are not readily prepared on their own. The similarity in the properties of PANI and PEDOT polymers did not require the removal of the "template" polymer after nanostructures formation. The presence of a PEDOT outer layer was confirmed by IR, Raman and XRD. The PEDOT layer significantly increased the room temperature electrical conductivity of the PEDOT/PANI nanocomposites by 2 orders of magnitude in comparison with regular PANI nanostructures. The PEDOT/PANI cast film electrode exhibited very good electrochemical activity toward the oxidation of ascorbic acid. The electrochemical activity and high conductivity of PEDOT/PANI nanorods, provided by PEDOT layer, may therefore allow the use of these nanostructured materials in electrochemical sensors in biomedical applications and in polymer electronics components and devices.

Acknowledgment. The authors gratefully acknowledge a University of Auckland Research Committee grant (No. 3606261) and the New Zealand Foundation for Science and Technology (Contract No. UOAX0408).

References and Notes

(1) MacDiarmid, A. G. *Angew. Chem., Int. Ed.* **2001**, *40*, 2581.
(2) Ramanavicius, A.; Ramanaviciene, A.; Malinauskas, A. *Electrochim. Acta* **2006**, *51*, 6025.
(3) Blinova, N. V.; Stejskal, J.; Trchova, M.; Prokes, J. *Polymer* **2006**, *47*, 42.
(4) Karlsson, K. F.; Aasberg, P.; Nilsson, K. P. R.; Inganaes, O. *Chem. Mater.* **2005**, *17*, 4204.
(5) Kang, S. K.; Kim, J.-H.; An, J.; Lee, E. K.; Cha, J.; Lim, G.; Park, Y. S.; Chung, D. J. *Polym. J.* **2004**, *36*, 937.
(6) Virji, S.; Huang, J.; Kaner, R. B.; Weiller, B. H. *Nano Lett.* **2004**, *4*, 491.
(7) Huang, K.; Wan, M.; Long, Y.; Chen, Z.; Wei, Y. *Synth. Met.* **2005**, *155*, 495.
(8) Bhandari, S.; Deepa, M.; Singh, S.; Gupta, G.; Kant, R. *Electrochim. Acta* **2008**, *53*, 3189.
(9) Abidian, M. R.; Kim, D.-H.; Martin, D. C. *Adv. Mater.* **2006**, *18*, 405.
(10) Parthasarathy, A.; Brumlik, C. J.; Martin, C. R.; Collins, G. E. *J. Membr. Sci.* **1994**, *94*, 249.
(11) Stejskal, J. *Microspheres, Microcapsules Liposomes* **2002**, *5*, 195.
(12) Steinhart, M.; Wendorff, J. H.; Greiner, A.; Wehrspohn, R. B.; Nielsch, K.; Schilling, J.; Choi, J.; Goesele, U. *Science* **2002**, *296*, 1997.
(13) Huang, J.; Virji, S.; Weiller, B. H.; Kaner, R. B. *J. Am. Chem. Soc.* **2003**, *125*, 314.
(14) Zhang, L.; Wan, M.; Wei, Y. *Macromol. Rapid Commun.* **2006**, *27*, 366.
(15) Xia, Y.; Yun, L. *Compos. Sci. Technol.* **2008**, *68*, 1471.
(16) Shim, G. H.; Han, M. G.; Sharp-Norton, J. C.; Creager, S. E.; Foulger, S. H. *J. Mater. Chem.* **2008**, *18*, 594.
(17) Peng, C.; Jin, J.; Chen, G. Z. *Electrochim. Acta* **2007**, *53*, 525.
(18) Lefrant, S.; Baibarac, M.; Baltog, I. *Mol. Cryst. Liq. Cryst.* **2006**, *447*, 393.
(19) Randriamahazaka, H.; Noel, V.; Guillerez, S.; Chevrot, C. *J. Electroanal. Chem.* **2005**, *585*, 157.
(20) Kvarnstrom, C.; Neugebauer, H.; Blomquist, S.; Ahonen, H. J.; Kankare, J.; Ivaska, A.; Sariciftci, N. S. *Synth. Met.* **1999**, *101*, 66.
(21) Lefebvre, M.; Qi, Z.; Rana, D.; Pickup, P. G. *Chem. Mater.* **1999**, *11*, 262.
(22) Abidian, M. R.; Martin, D. C. *Biomaterials* **2008**, *29*, 1273.
(23) Vasantha, V. S.; Chen, S.-M. *J. Electroanal. Chem.* **2006**, *592*, 77.
(24) Kumar, S. S.; Mathiyarasu, J.; Phani, K. L.; Jain, Y. K.; Yegnaraman, V. *Electroanalysis* **2005**, *17*, 2281.
(25) Bello, A.; Giannetto, M.; Mori, G.; Seeber, R.; Terzi, F.; Zanardi, C. *Sens. Actuators, B* **2007**, *B121*, 430.
(26) Seo, K. I.; Chung, I. J. *Polymer* **2000**, *41*, 4491.
(27) Chiu, W. W.; Travas-Sejdic, J.; Cooney, R. P.; Bowmaker, G. A. *Synth. Met.* **2005**, *155*, 80.
(28) Sapurina, I. Y.; Stejskal, J.; Trchova, M.; Hlavata, D.; Biryulin, Y. F. *Fullerenes, Nanotubes, Carbon Nanostruct.* **2006**, *14*, 447.
(29) Fu, Y.; Elsenbaumer, R. L. *Chem. Mater.* **1994**, *6*, 671.
(30) Huh, P.-H.; Kim, S.-C.; Kim, Y.-H.; Kumar, J.; Kim, B.-S.; Jo, N.-J.; Lee, J.-O. *Polym. Eng. Sci.* **2007**, *47*, 71.
(31) Jang, J.; Chang, M.; Yoon, H. *Adv. Mater.* **2005**, *17*, 1616.
(32) Trchova, M.; Sedenkova, I.; Stejskal, J. *Synth. Met.* **2005**, *154*, 1.
(33) Zhang, L.; Peng, H.; Hsu, C. F.; Kilmartin, P. A.; Travas-Sejdic, J. *Nanotechnology* **2007**, *18*, 115607/1.
(34) Trchova, M.; Sedenkova, I.; Konyushenko, E. N.; Stejskal, J.; Holler, P.; Ciric-Marjanovic, G. *J. Phys. Chem. B* **2006**, *110*, 9461.
(35) Stejskal, J.; Sapurina, I.; Trchova, M.; Konyushenko, E. N.; Holler, P. *Polymer* **2006**, *47*, 8253.
(36) Liu, W.; Kumar, J.; Tripathy, S.; Senecal, K. J.; Samuelson, L. *J. Am. Chem. Soc.* **1999**, *121*, 71.
(37) Huang, J.; Wan, M. *J. Polym. Sci., Part A: Polym. Chem.* **1999**, *37*, 151.
(38) Kvarnstrom, C.; Neugebauer, H.; Ivaska, A.; Sariciftci, N. S. *J. Mol. Struct.* **2000**, *521*, 271.
(39) Damlin, P.; Kvarnstrom, C.; Ivaska, A. *J. Electroanal. Chem.* **2004**, *570*, 113.
(40) Bernard, M.-C.; Hugot-Le Goff, A. *Synth. Met.* **1997**, *85*, 1145.
(41) Gruger, A.; Novak, A.; Regis, A.; Colomban, P. *J. Mol. Struct.* **1994**, *328*, 153.
(42) Sariciftci, N. S.; Bartonek, M.; Kuzmany, H.; Neugebauer, H.; Neckel, A. *Synth. Met.* **1989**, *29*, E193.
(43) Pereira da Silva, J. E.; Cordoba de Torresi, S. I.; de Faria, D. L. A.; Temperini, M. L. A. *Synth. Met.* **1999**, *101*, 834.
(44) Chiu, W. W.; Travas-Sejdic, J.; Cooney, R. P.; Bowmaker, G. A. *J. Raman Spectrosc.* **2006**, *37*, 1354.
(45) Sakamoto, S.; Okumura, M.; Zhao, Z.; Furukawa, Y. *Chem. Phys. Lett.* **2005**, *412*, 395.
(46) Garreau, S.; Louarn, G.; Buisson, J. P.; Froyer, G.; Lefrant, S. *Macromolecules* **1999**, *32*, 6807.
(47) Garreau, S.; Louam, G.; Lefrant, S.; Buisson, J. P.; Froyer, G. *Synth. Met.* **1999**, *101*, 312.
(48) Im, S. G.; Gleason, K. K. *Macromolecules* **2007**, *40*, 6552.
(49) Garreau, S.; Duvail, J. L.; Louarn, G. *Synth. Met.* **2001**, *125*, 325.
(50) Zhang, L.; Wan, M. *Thin Solid Films* **2005**, *477*, 24.
(51) Wei, Z.; Zhang, Z.; Wan, M. *Langmuir* **2002**, *18*, 917.
(52) Gong, J.; Su, Z. M.; Dai, Z. M.; Wang, R. S.; Qu, L. Y. *Synth. Met.* **1999**, *101*, 751.
(53) Choi, J. W.; Han, M. G.; Kim, S. Y.; Oh, S. G.; Im, S. S. *Synth. Met.* **2004**, *141*, 293.
(54) Goncalves, D.; dos Santos, D. S., Jr.; Mattoso, L. H. C.; Karasz, F. E.; Akcelrud, L.; Faria, R. M. *Synth. Met.* **1997**, *90*, 5.
(55) Weidlich, C.; Mangold, K. M.; Juettner, K. *Electrochim. Acta* **2005**, *50*, 1547.
(56) Zhang, L. *J Solid State Electrochem* **2007**, *11*, 365.
(57) Pauliukaite, R.; Brett, C. M. A.; Monkman, A. P. *Electrochim. Acta* **2004**, *50*, 159.
(58) Takashima, W.; Nakashima, M.; Pandey, S. S.; Kaneto, K. *Electrochim. Acta* **2004**, *49*, 4239.
(59) Kilmartin, P. A.; Martinez, A.; Bartlett, P. N. *Curr. Appl. Phys.* **2008**, *8*, 320.

MA8013228